Progress in Nuclear Energy 90 (2016) 11–18

Contents lists available at ScienceDirect

Progress in Nuclear Energy

journal homepage: www.elsevier.com/locate/pnucene

Natural circulation characteristics of lead-based reactor under long-term decay heat removal

Xiaojuan Wang, Ming Jin, Guowei Wu, Yong Song, Yazhou Li, Yunqing Bai*

Key Laboratory of Neutronics and Radiation Safety, Institute of Nuclear Energy Safety Technology, Chinese Academy of Sciences, Hefei, Anhui, 230031, China

ARTICLE INFO

Article history:
Received 29 September 2015
Received in revised form
5 February 2016
Accepted 9 February 2016
Available online 5 March 2016

Keywords:
China Lead-based Research Reactor (CLEAR-I)
RVACS
Primary heat exchangers (PHXs) cooling system
Natural circulation

ABSTRACT

The natural circulation of primary coolant plays an important role in removing the decay heat in Station-Black-out (SBO) accident from reactor core to decay heat removal systems, such as RVACS and PHXS cooling, for lead-based reactor. In order to study the natural circulation characteristics of primary coolant under Reactor Vessel Air Cooling System (RVACS) and primary heat exchangers (PHXs) cooling, which are crucial to the safety of lead-based reactors. A three-dimensional CFD model for the China Lead-based Research Reactor (CLEAR-I) has been built to analyze the thermal-hydraulics characteristics of primary coolant system and the cooling capability of the two systems. The abilities of the two cooling systems with different decay heat powers were discussed as well. The results demonstrated that the decay heat could be removed effectively only relying on either of the two systems. However, RVACS appeared the obvious thermal stratification phenomenon in the cold pool. Besides, with the increase in decay heat power, the natural circulation capacity of primary coolant between the two systems had a significant difference. The PHXs cooling system was stronger than the RVACS, with respect to the mass flow of primary coolant and the average temperature difference between cold pool and hot pool.

1. Introduction

As a fast reactor system, the Lead-based reactors are particularly effective in fuel utilization as well as for burning long-life actinide components of high-level waste, that have accumulated from past and ongoing Generation I through III nuclear fuel cycles (Wu, 2006, 2009a; Wu et al., 1999). Motived by above good properties of Lead-based reactors, a great deal of interests have been displayed in Lead or LBE cooled fast reactors (Wu et al., 2008; Huang et al., 2004, 2009a). Chinese Academy of Sciences (CAS) launched an engineering project to develop Accelerator Driven System (ADS) for nuclear waste transmutation since 2011 (Wu et al., 2002; Wu, 2009b). China Lead-based Research Reactor (CLEAR-I) proposed by Institute of Nuclear Energy Safety Technology (INEST) was selected as the reference reactor in this ADS project (Huang et al., 2009b, 2013; Wu et al., 2015a; Song et al., 2014).

The Reactor Vessel Air Cooling System (RVACS) that removing the decay heat in the typical Station-Black-out (SBO) accident is one of the most important approaches to increase the safety of Lead-based reactors. Many countries applied this system for their lead or lead–alloy cooled fast reactor (LFR), such as MYRRHA, SSTAR and SVBR (Song et al., 2014), etc. Meanwhile, the primary heat exchangers (PHXs) cooling system as one of passive decay heat system could remove the decay heat when primary coolant flowed through the PHXs where pressurized water in secondary loops was heated into vapor without the power supply. The Belgian Nuclear Research Center (SCK-CEN) has applied the passive PHXs cooling system in the MYRRHA (Maes, 2006). CLEAR-I adopted the two varieties of passive decay heat removal systems, which are RVACS and PHXs cooling.

In this paper, a three-dimensional model based on CLEAR-I was established, and the velocity and temperature distribution of primary coolant under long-term decay heat removal condition was simulated. One of the objectives of this work was the study on the natural circulation characteristics of primary coolant in which the RVACS and PHXs cooling system was initiated, during the SBO accident without using any external power supply, respectively. Meanwhile, the capacity of two systems was compared based on different decay heat powers.

* Corresponding author.
E-mail address: yunqing.bai@fds.org.cn (Y. Bai).

http://dx.doi.org/10.1016/j.pnucene.2016.02.009
0149-1970/

2. CLEAR-I design description

The CLEAR-I is a pool type reactor which was proposed by FDS team for Accelerator Driven Subcritical System (Wu et al., 2016). It is an experimental reactor for thermal-hydraulics, neutronics and safety analysis. The lead-bismuth eutectic which flows through the core, hot pool, cold pool, four PHXs and two pumps consist of the primary coolant system. A heat barrier separates hot pool and cold pool. The cold pool incorporates two primary pumps which drive the fluid flow the core when the reactor is in normal operation. The RVACS placed outside of the reactor safety vessel. The configuration of the CLEAR-I has shown in Fig. 1, the main design parameters presented in Table 1, furthermore, the thermal power of the CLEAR-I is 10 MW and average inlet and outlet temperature of the core is 300 °C and 385 °C respectively (Wu et al., 2015b; Sheng et al., 2014).

3. Calculation model

3.1. Geometry model

A simplified model of CLEAR-I which the height and diameter is 6.8 m and 4.6 m respectively has been established, as shown in Fig. 2. Since the layout of the internal structures in the reactor is complicated, especially the construction of core, it is impractical to model the all subassemblies arrangement. Some simplifications are needed to be done as follows: firstly, the model assumed a cylinder for core in place of 86 fuel assemblies with different enrichment zones; then the four PHXs are simulated as annular model and the secondary side tubes are neglected; additionally, fuel handling machine located in the cold pool has small influence in the study, therefore, it can be neglected as well. The simplified geometry model has been meshed following a block-structured strategy, and the quantity of blocks are 2892.

3.2. Grid sensitivity analysis

In this paper investigated the effect of grid sensitivity analysis based on different mesh levels to the coolant flow in the above-mentioned model. This grid sensitivity analysis was performed based on three different grids: a finer grid, a coarser grid and a reference grid. The different temperature output of core outlet for different mesh value with the same boundary conditions are extracted and plotted in the Fig. 3. It indicates that both the values of 3 million and 5 million mesh sizes were consistent. Obliviously, the 2 million mesh was not in accordance with the two other.

1. Safety vessel
2. Manifold
3. Reactor core
4. Primary pump
5. Control rod driven system
6. PHXs
7. RVACS
8. Cover

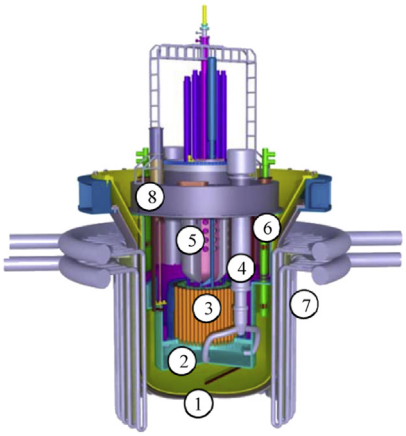

Fig. 1. The configuration of the CLEAR-I.

Table 1
CLEAR-I main parameters.

Parameters	Value
Thermal power (MW)	10
Core inlet/outlet temperature (°C)	300/385
Primary coolant mass flow rate (kg/s)	811.67
Total LBE coolant(t)	~600
Fuel assembly	86

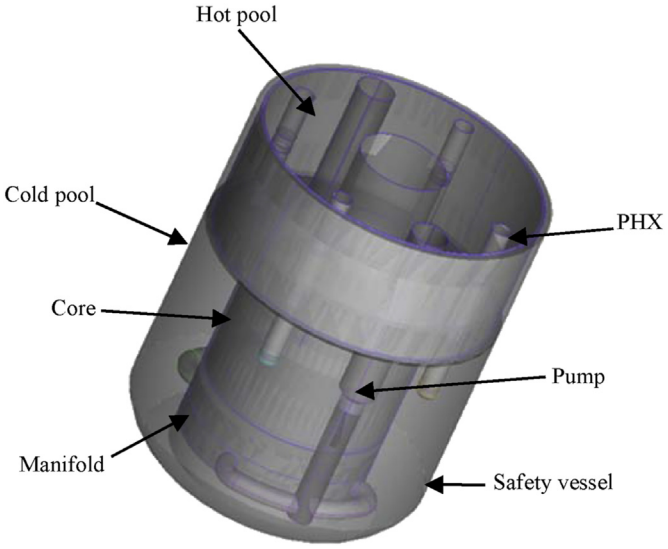

Fig. 2. The simplified geometry model of CLEAR-I.

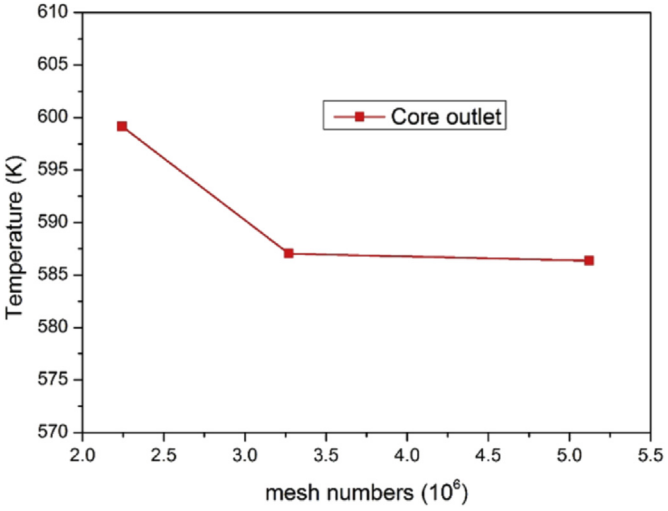

Fig. 3. The core outlet temperature for different mesh levels.

However, in consideration of the computational time and the performance of computers, the 3.271128 million mesh was selected.

3.3. Porous medium approach

In the geometry model, the configurations of core and PHXs have been simplified while the two parts implies a significant effect on the pressure loss of primary coolant. Therefore, porous medium model has been applied to realize the same pressure drop as the real flow. The pressure drop was modeled by the porous medium

Table 2
Thermal-hydraulics parameters comparison of design and calculation values.

Parameters	Design	CFD simulation	Relative error (%)
Average core inlet temperature (K)	573.0	573.1	0.02
Average core outlet temperature (K)	658.0	654.1	0.6
Coolant mass flow (kg/s)	811.7	817.3	0.7

approach are in accordance with the pressure drop calculated by the thermal-hydraulics design and analysis in different Reynolds number.

3.4. Turbulence model

For the liquid metals, the ReNormalization Group (RNG) methodology can simulate its special turbulent behavior and has been confirmed by experimental data for liquid sodium (Zhao et al., 2015; Vanderhaegena and et al., 2011). Thus the k-ε model which relates to the turbulent kinetic energy (k) and the turbulent dissipation rate (ε), could simulate the liquid metal thermal-hydraulic behavior and was selected as the turbulence model (Todreas and Kazimi, 1990; Lin et al., 2000). Besides, the turbulence model is supplied with standard wall functions, since the boundary condition was simulated by adiabatic except for the reactor vessel is a heat flux boundary condition in the calculation model for RVACS. The LBE properties in the simulation were referred to the LBE handbook (OECD/NEA Nuclear Science Committee, 2007).

3.5. Steady state discussion

The steady state simulation of the computational model was carried out in BOC (beginning of cycle) condition using CFD code. Major thermal-hydraulics parameters were listed and compared with the design values in Table 2. As shown in Table 2, the values calculated by the computational model fit in with designed values, and the relative error were all less than 1%. The primary coolant temperature distribution of the computational model was presented in Fig. 4.

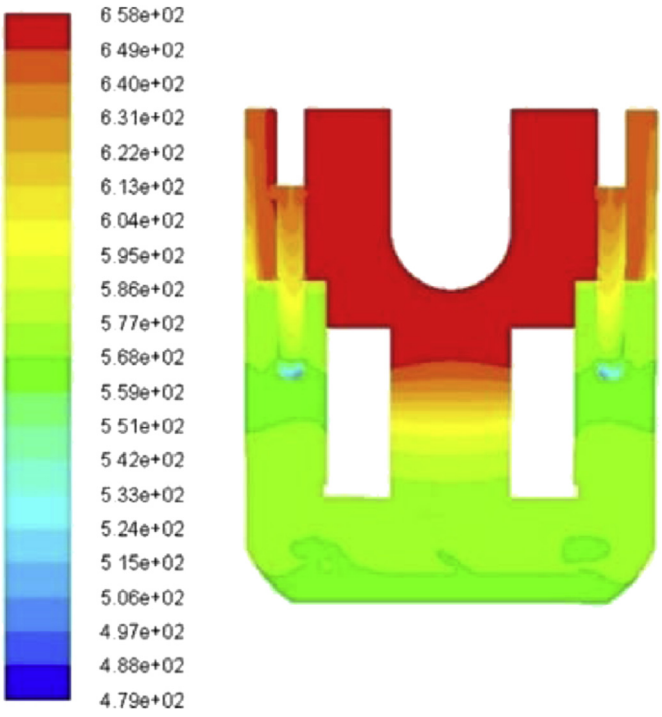

Fig. 4. The primary coolant temperature distribution of the computational model.

3.6. Boundary conditions

3.6.1. RVACS cooling

Fig. 5 shows the RVACS working diagram, The RVACS is a natural circulation cooling system and consists of air collector tubes installed in the reactor vault. The air collector tubes are full with air and the air is driven by natural circulation to keep the concrete temperature below the design limit. For the CLEAR-I, the RVACS could extract 0.1 MW with the safety vessel average temperature at 216.2 °C and main vessel temperature at 304.6 °C (Wu et al., 2016).

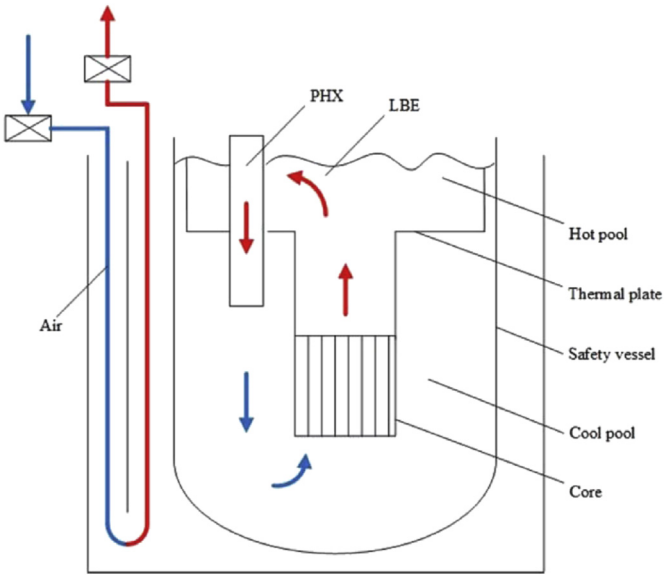

Fig. 5. The working diagram of RVACS.

According to preliminary analysis, a multiple-term formula between removing decay heat and temperature has already been evaluated (Wu et al., 2015b),

$$Q = 1773.59 - 12.4556 \times T + 0.03737 \times T^2 - 0.0000471937 \times T^3 \quad (1)$$

where Q refers to the RVACS heat flux, T is the safety vessel wall temperature.

So for the present work, the heat flux of RVACS is simulated according to the above formula which depends on the changed safety vessel wall temperature and is simulated through using the UDF in ANSYS Fluent. The decay heat power of the core is set as the constant 1% of nominal power (0.1 MW) for a long term.

3.6.2. PHXs cooling

The working diagram of PHXs cooling system shows in Fig. 6. For the CLEAR-I, each PHX could remove about 2.5 MW heat at the normal operating condition. Nevertheless, in the reactor shutdown condition, the PHXs cooling system could cooling the reactor without external power supply and only depends on the natural circulation of secondary loop coolant. In the worst case, the

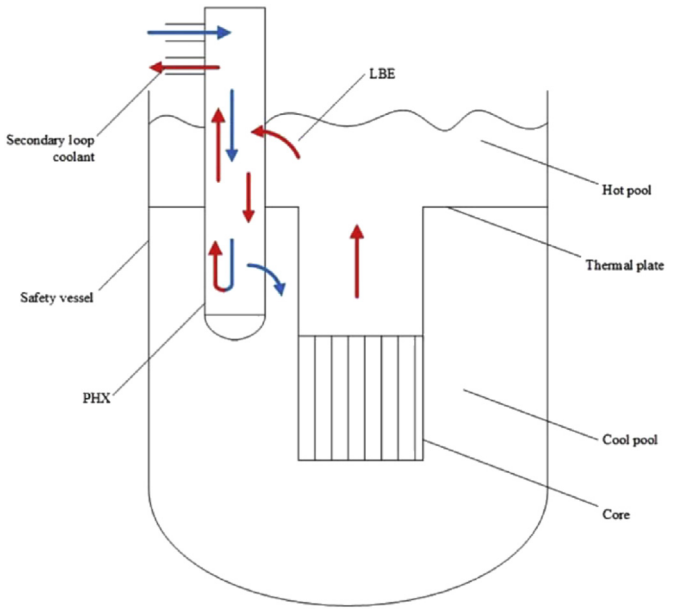

Fig. 6. The working diagram of PHXs cooling system.

pressurized water (4 MPa) was heated into water vapor in the PHXs and then comes back to the PHXs when condensates into liquid water. In this way, the decay heat was removed.

In this paper, the temperature of pressurized water was conservatively supposed as the boiling point (250 °C) of pressurized water. Based on the average temperature of the inlet pressurized water and the fixed inlet and outlet LBE temperature under the normal operating condition, a source term of PHXs is followed as (Zhao et al., 2015):

$$Q = -\frac{10MW}{0.73} \times \frac{T_{ave} - 523}{119} \tag{2}$$

where the Q is the total volume of heat exchanging region, and the T_{ave} is the averaged LBE temperature at the PHX region. The decay heat power was set same as the RVACS.

4. Results and discussion

4.1. RVACS cooling

The temperature distribution at the symmetry plane of the pump and the PHXs with RVACS are given in Fig. 7, respectively. As can be seen in Fig. 7, the minimum and maximum temperature in the vessel was respectively 247 °C and 254 °C. The coolant temperature in the hot pool is nearly same with the core region, however, the cold pool generated the apparent thermal stratification phenomenon. We can see from the Fig. 7 that the cold pool temperature gradually decreasing from the upper to the bottom. It was because that the upper part of cold pool which surrounds the hot pool was narrow, which were about 10 cm and the coolant here relatively small. When it was heated by the thermal plate outside the hot pool, there was no enough distance to remove the heat at once.

Fig. 8 shows the detail temperature and velocity distribution in the upper part of cold pool. The limited coolant located in this section was cooled by safety vessel wall and the other side was heated by thermal plate wall. Hence the coolant in this section performed the convection flow which exactly as Fig. 8 shows. It could also explain that the temperature in the upper part was higher than that of the other parts.

Besides, from Fig. 7 we can see that in the region of manifold, the temperature seems above the cold pool. It is because the thermal conductivity of LBE is high (12 $W/m^{-1}K^{-1}$ at 300 °C), while the velocity under the reactor shutdown condition is low, only 0.006 m/s. So the effect of thermal conductivity is far over the thermal convection. Therefore, the coolant in the manifold has been heated by the conduction by the core coolant before the cold coolant in the cold pool flowed into the manifold.

A closer look in the region of PHX is shown in Fig. 9; we can see that the primary coolant that has flowed out from the outlet of PHXs directly flowed upward. Due to the big temperature difference between PHX outlet and cold pool, the heated coolant from

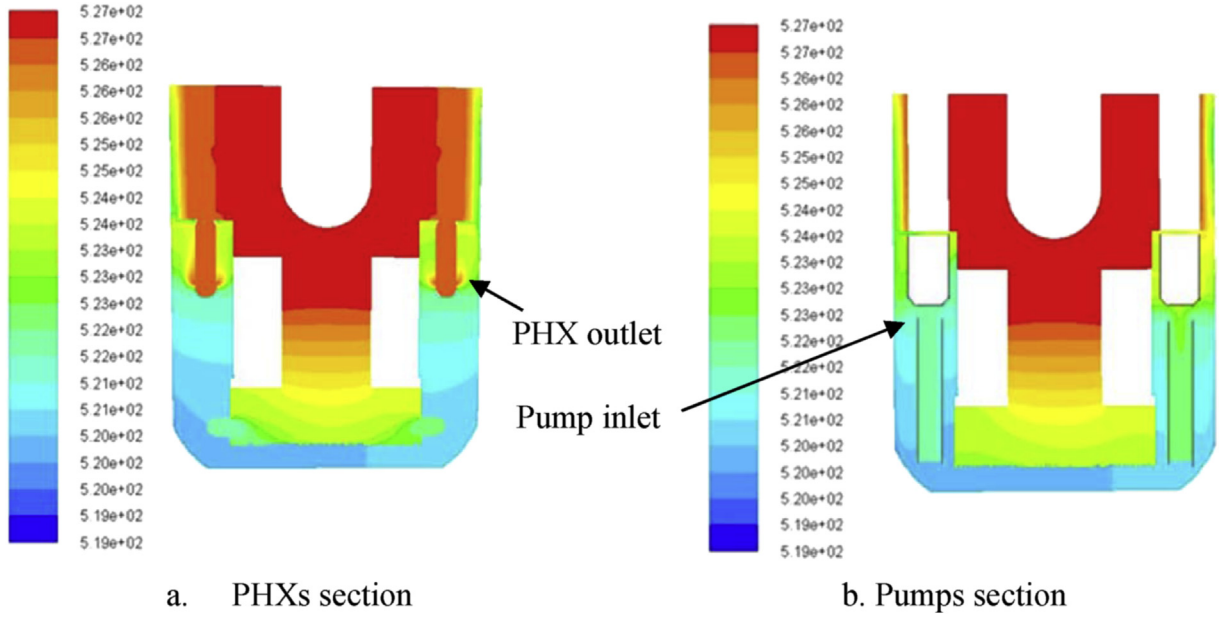

Fig. 7. The temperature distribution at the symmetry plane of the pump and the PHXs with RVACS.

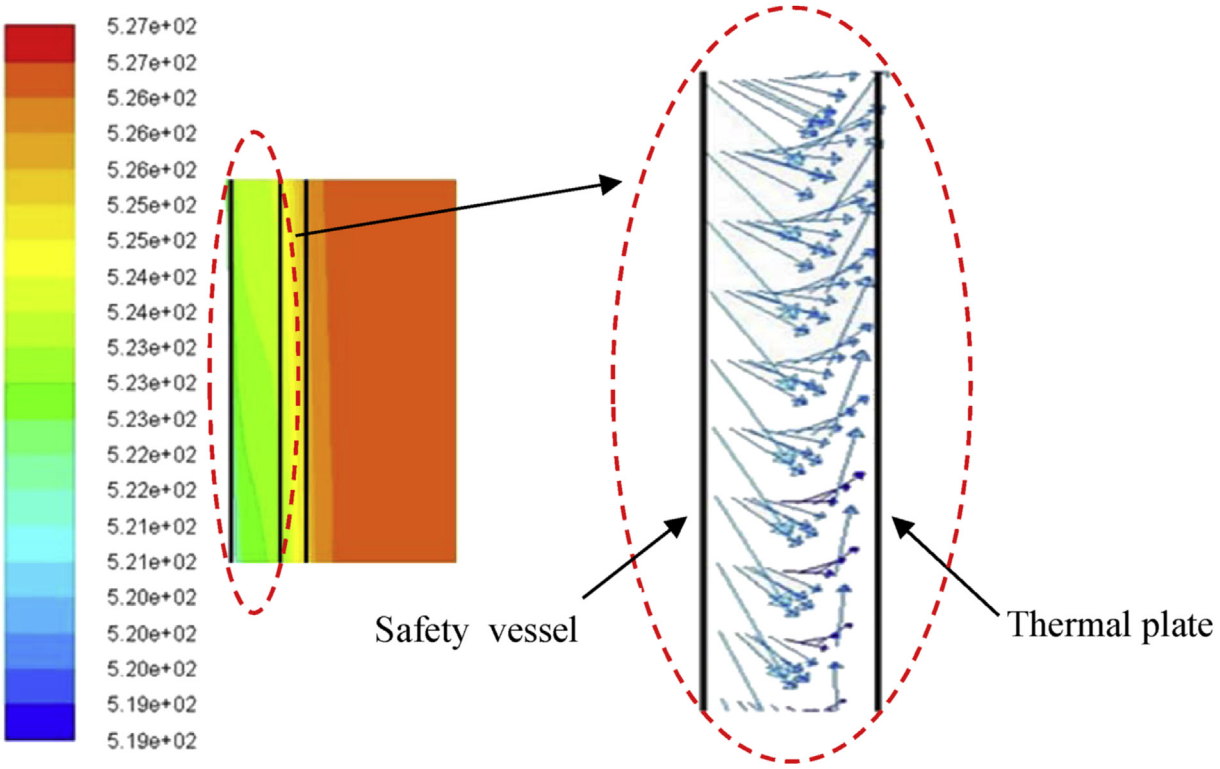

Fig. 8. The temperature and velocity distribution in the upper part of cold pool.

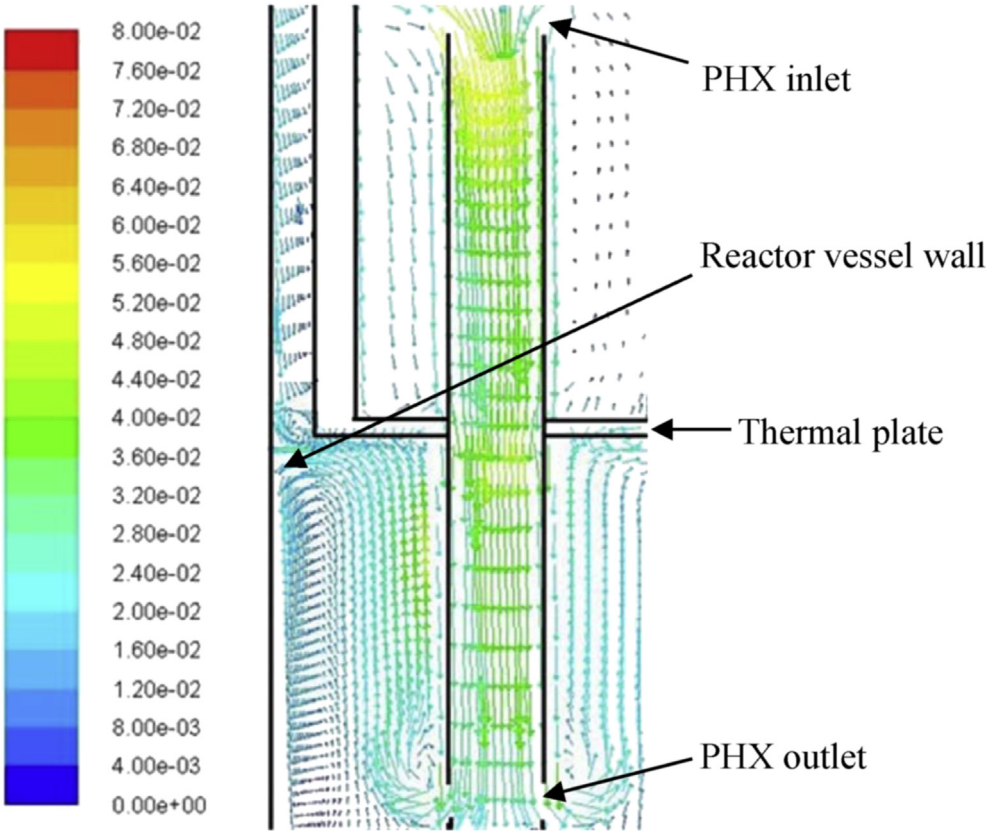

Fig. 9. The velocity of PHXs section.

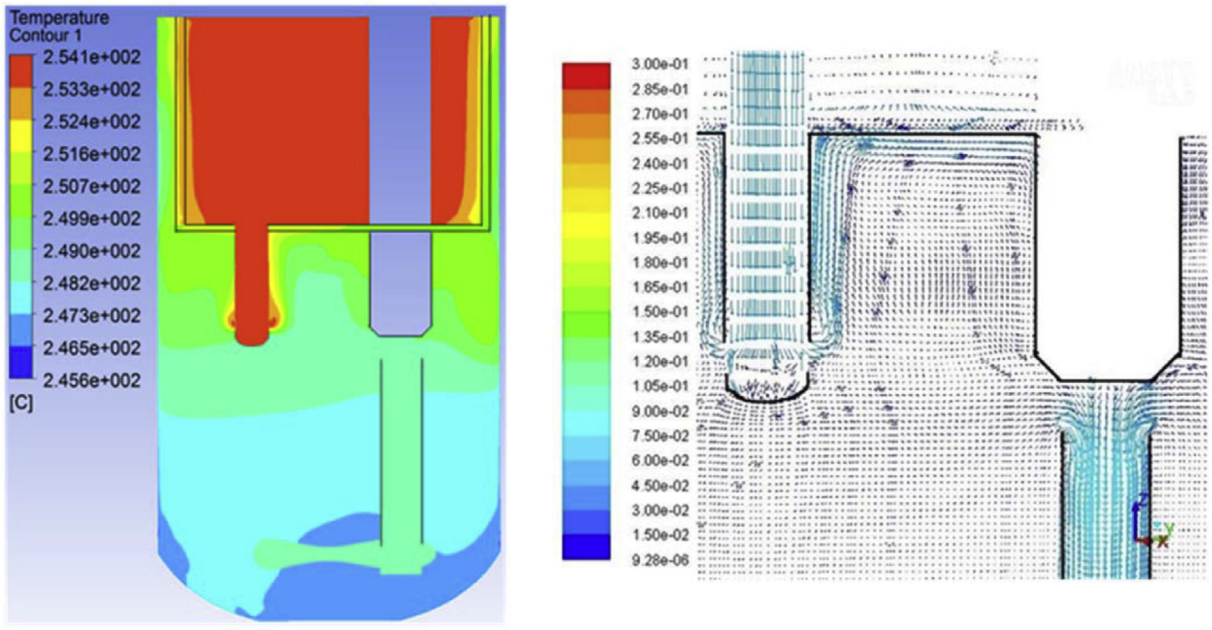

Fig. 10. The temperature and velocity distribution in the region between the heat exchanger and pump.

the PHX outlet flowed upward by buoyancy effects and arrived at the bottom of the thermal plate. Fig. 10 shows the temperature and velocity distribution of the symmetry plane of a PHX-pump section. It can be seen that the liquid flowed along the thermal plate and then flowed down. Additionally, the coolant has entered into the pump before flowed into the other parts of cold pool, especially the bottom cooled liquid regions. However, the RVACS transfers heat through the safety vessel which surrounds the cold pool, which need the fully flow of primary coolant, so this coolant flow could not realize the effective heat transfer of RVACS. Based on this, we can consider that reducing the height of the inlet of pumps could achieve effectively cooling. So the improvement for the design of CLEAR-I could take into account the above-mentioned facts in the future work.

4.2. PHXs cooling

Fig. 11 shows the temperature distribution with PHXs cooling. The associated velocity distribution is given in Fig. 12. The temperature and velocity distribution in the hot pool was nearly homogeneous, and the LBE temperature reduced when flowed into the PHXs. However, contracted to the RVACS cooling, obviously, the cold pool had not the thermal stratification phenomenon.

At the bottom of the PHXs, the temperature was significantly

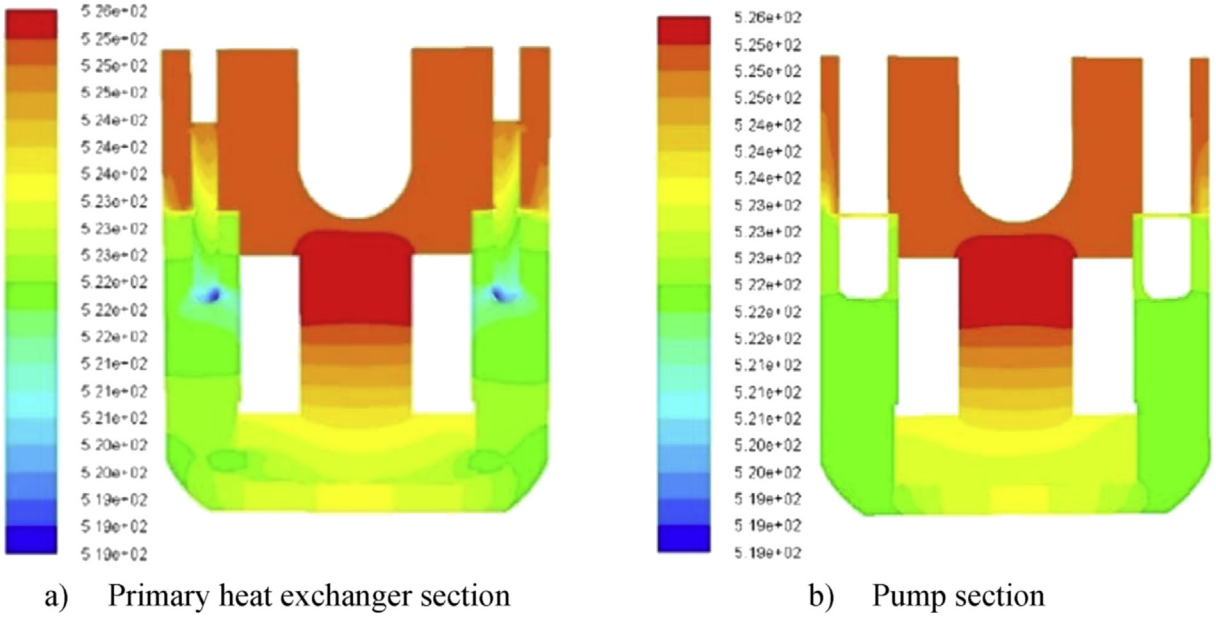

Fig. 11. The temperature distribution at the symmetry plane of the pump and the PHXs with PHXs cooling.

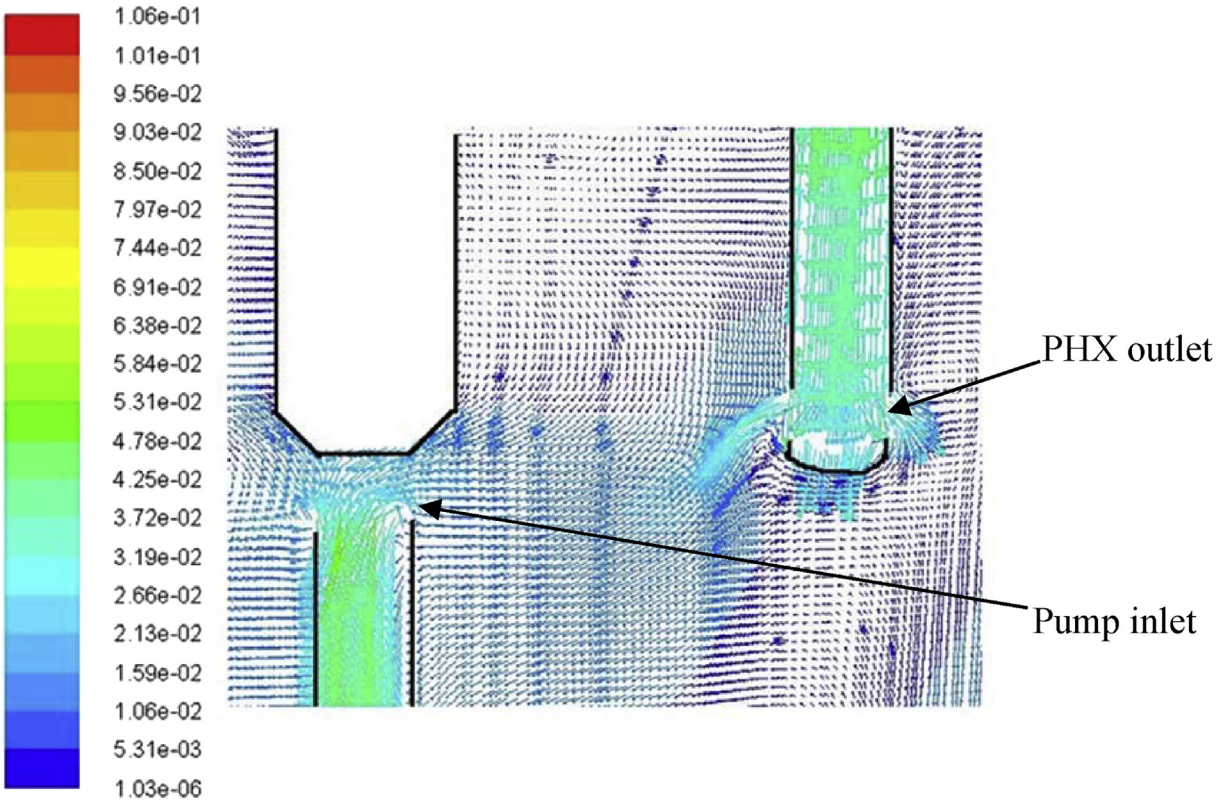

Fig. 12. The velocity distribution of PHXs cooling.

lower than that of other zones. It can be identified from Fig. 12 that the stagnancy of flow existed in this location. The outlet of PHXs was annular and was located above the bottom of the PHXs. The cause for this stagnancy is the primary coolant directly flowed out from the outlet of PHXs without fully flowing in the bottom of the PHXs.

From the Fig. 12 we can also see that the flow in the plane of PHX-pump section was different from the RVACS, apparently, the coolant that flowed from the outlet of PHXs directly flowed downward which was significantly from the RVACS. As mention above, for the RVACS, there were obvious coolant temperature difference between PHX outlet and cold pool, which was almost non-existent for PHXs cooling. The liquid flowed into the cold pool whose temperature was in same level with the interior of PHX, and thus flowed down without the buoyancy effect. It also can be seen from the Fig. 12 that the coolant in the cold pool medium part where located between PHX outlet and pump inlet appeared cross flow phenomenon and flowed into the pump once met the pump inlet.

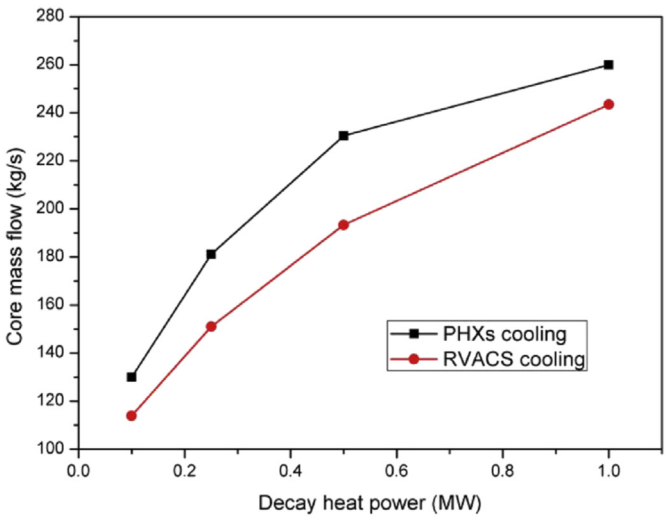

Fig. 13. The core mass flow of two cooling systems.

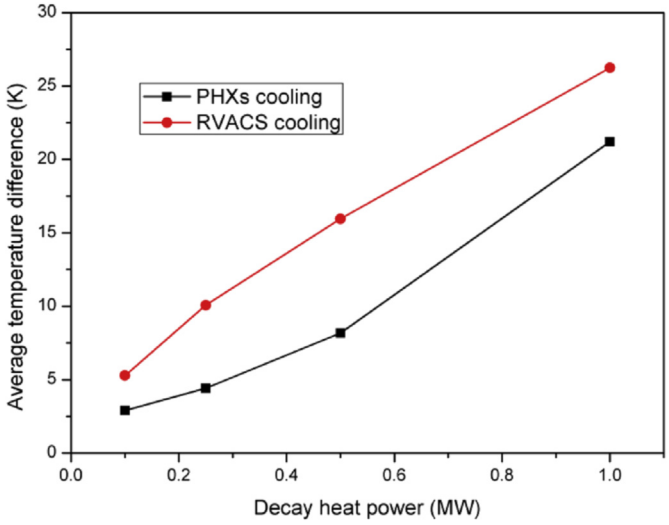

Fig. 14. The average temperature difference between hot pool and cold pool.

4.3. Comparison and discussion

From the above results, we can consider that the stable natural circulation of primary coolant could be formed with the two cooling systems and the decay heat of CLEAR-I could be taken away. The maximum temperature was far below the acceptable value of the reactor components.

However, to explore the difference of two cooling systems, the different decay heat power was simulated to contrast the natural circulation capacity. Fig. 13 shows the core mass flow with different decay heat power. We can see that the core mass flow of PHXs cooling system was always larger than the RVACS as the decay heat power increasing. The average temperature difference between cold pool and hot pool was shown in Fig. 14, the temperature difference for PHXs cooling was smaller than RVACS which was opposed to the above mass flow graph, and the temperature distribution in the PHXs cooling was more homogeneous than the RVACS. For PHXs cooling, the heat transfer ability depends on the phase change of secondary loop coolant which pressurized water boils (less than 300 °C, for the CLEAR-I about 250 °C) and turns into steam in PHXs. While the RVACS cools the safety vessel firstly and then remove the decay heat through the natural circulation of primary coolant. Therefore, the RVACS cooling capacity depends upon the design of CLEAR-I external units to realize the optimal removing decay heat effects.

5. Conclusion

A three-dimensional simplified CFD model for CLEAR-I was built to study natural circulation characteristics of primary coolant under long-term decay heat removal condition with RVACS and PHXs cooling system. Through the numerical simulation, the temperature and velocity distribution in the primary coolant system were illustrated and discussed. The steady natural circulation was established under two conditions with the acceptable coolant temperatures.

The thermal stratification appeared in the cold pool with RVACS which the primary coolant flowed upward from the PHX outlet because of buoyancy effect. Flow convection was established in the upper part of cold pool where liquid was heated by thermal plate with one side and another side was cooled by reactor vessel. For PHXs cooling, the cold pool temperature was well-distributed and the velocity in the reactor was bigger.

Additionally, the difference between PHXs cooling system and RVACS was investigated in this contribution. The PHXs cooling system could better remove the decay heat than the RVACS in the different decay power level. The core mass flow for PHXs cooling was larger than the RVACS, and temperature difference between cold pool and hot pool was smaller, meanwhile, the temperature distribution in the cold pool was more homogeneous.

Acknowledgments

The authors appreciate the efforts of the other members in FDS Team, as well as the Strategic Priority Research Program of the Chinese Academy of Sciences (Grant No.XDA03040000).

References

Huang, Q., Li, J., Chen, Y., 2004. Study of irradiation effects in china low activation martensitic steel CLAM. J. Nucl. Mater 329, 268–272.
Huang, Q., Gao, S., Zhu, Z., Zhang, M., Song, Y., Li, C., Chen, Y., Ling, X., Zhou, X., 2009a. Progress in compatibility experiments on lithium–lead with candidate structural materials for fusion in China. FDS Team Fusion Eng. Des. 84, 242–246.
Huang, Q., Wu, Y., Li, J., Wan, F., Chen, J., Luo, G., Liu, X., Chen, J., Xu, Z., Zhou, X., Ju, X., Shan, Y., Yu, J., Zhu, S., Zhang, P., Yang, J., Chen, X., Dong, S., 2009b. Status and Strategy of fusion materials development in China. J. Nucl. Mater. 386–388, 400–404.
Huang, Q., Baluc, N., Dai, Y., Jitsukawa, S., Kimura, A., Konys, J., Kurtz, R.J., Lindau, R., Muroga, T., Odette, G.R., Raj, B., Stoller, R.E., Tan, L., Tanigawa, H., Tavassoli, A.-A.F., Yamamoto, T., Wan, F., Wu, Y., 2013. Recent progress of R&D activities on reduced activation ferritic/martensitic steels. J. Nucl. Mater. 442 (1–3), S2–S8.
Lin, B.-S., Chang, C.C., Want, C.-T., 2000. Renormalization group analysis for thermal turbulent transport. Phys. Rev. E 63 (016304), 1–11.
Maes, Dirk, 2006. Mechanical design of the small-scale experimental ADS: MYRRHA. Energy Convers. Manag. 47, 2710–2723.
Sheng, Meiling, Ming, Jin, Yunqing, Bai, Weihua, Wang, Yican, Wu, FDS Team, 2014. Preliminary design and analysis of emergency decay heat removal system for China lead alloy cooled research reactor. Chin. J. Nucl. Sci. Eng. 34, 91–96.
Song, J., Sun, G., Chen, Z., Zheng, H., Hu, L., 2014. Benchmarking of CAD-based SuperMC with ITER benchmark model. Fusion Eng. Des. 89, 2499–2503.
Todreas, N.E., Kazimi, M.S., 1990. Nuclear Systems I – Thermal Hydraulic Fundamen-tals. Tayler& Francis.
Vanderhaegena, M., et al., 2011. CFD analysis of the MYRRHA primary cooling system. Nucl. Eng. Des. 241, 775e784.
Working Group on Lead-BismuthEutectic OECD/NEA Nuclear Science Committee, 2007. Handbook on Lead-bismuth Eutectic Alloy and Lead Properties, Materials Compatibility, Thermal-hydraulics and Technologies, ISBN 978-92-64-99002-9.
Wu, Y., FDS Team, 2006. Conceptual design activities of FDS series fusion power plants in China. Fusion Eng. Des. 81, 2713–2718.
Wu, Y., FDS Team, 2009. CAD-Based interface programs for fusion neutron transport simulation. Fusion Eng. Des. 84, 1987–1992.
Wu, Y., FDS Team, 2009. Fusion-based hydrogen production reactor and its material selection. J. Nucl. Mater. 386–388, 122–126.
Wu, Y., Xie, Z., Fischer, U., 1999. A discrete ordinates nodal method for one-dimensional neutron transport calculation in curvilinear geometries. Nucl. Sci. Eng. 133, 350–357.
Wu, Y., Xiao, B., Xu, Q., Yu, J., 2002. The fusion-driven hybrid system and its material selection. J. Nucl. Mater. 307–311, 1629–1636.
Wu, Y., Song, G., Cao, R., Wu, A., Cheng, M., Tang, Z., Li, G., Jing, J., Liu, H., Li, J., Lan, H., Meng, Y., Zheng, H., Jin, C., Zeng, Q., Zheng, S., Huang, Q., Wu, L., Li, G., Lin, H., Tao, S., Shi, C., 2008. Development of accurate/advanced radiotherapy treatment planning and quality assurance system (ARTS). Chin. Phys. C (HEP& NP) 32, 177–182.
Wu, Y., Song, J., Zheng, H., Sun, G., Hao, L., Long, P., Hu, L., FDS Team, 2015. CAD-based Monte Carlo program for integrated simulation of nuclear system SuperMC. Ann. Nucl. Energy 82, 161–168.
Wu, Y., Bai, Y., Song, Y., et al., January 2016. Development strategy and conceptual design of china lead-based research reactor. Ann. Nucl. Energy 87 (Part 2), 511–516.
Wu, G., Jin, M., Chen, J., et al., 2015b. Assessment of RVACS performance for small size lead-cooled fast reactor. Ann. Nucl. Energy 77, 310–317.
Zhao, P., Li, S., et al., 2015. Natural circulation characteristics analysis of a small modular natural circulation lead-bismuth eutectic cooled fast reactor. Prog. Nucl. Energy 83, 220–228.